Structural Engineering and Mechanics, Vol. 4, No. 6 (1996) 655-678
DOI: http://dx.doi.org/10.12989/sem.1996.4.6.655

Non-conventional formulations for the finite element method

J. A. Teixeira de Freitas†, J. P. Moitinho de Almeida‡ and E. M. B. Ribeiro Pereira‡

Departamento de Engenharia Civil, Instituto Superior Técnico. Av. Rovisco Pais, 1096 Lisboa Codex, Portugal

Abstract. The paper reports on alternative hybrid/mixed formulations being developed by the Structural Analysis Research Group of Instituto Superior Técnico. These formulations open the scope and increase the power of the finite element method by allowing different fields to be independently approximated, within certain consistency criteria, and by enhancing the use of a wide range of approximation functions. They have been applied to the analysis of 2-D problems, laminar structures and solids, using different constitutive relations, both in quasi-static and dynamic regimes. The fundamental properties of the formulations are identified and assessed and their performance is illustrated using simple, linear applications.

Key words: hybrid; mixed; equilibrium and Trefftz finite elements.

1. Introduction

Although the basis for the development of hybrid and mixed formulations has long been established (Pian 1969), the hybrid and mixed finite elements never gained widespread acceptance. Several reasons have been evoked to justify this failure in their direct competition with the conventional, conforming finite element.

Some of these reasons derive from the advantages inherent to the conventional finite element formulation, namely simplicity of the supporting concepts, robustness, and ability to produce estimates with controlled accuracy for virtually every structural engineering problem. Other arguments focus directly on the weaknesses of the hybrid and mixed formulations: poorer performance-cost ratios, the difficulties associated with controlling the possible emergence of spurious modes and the possibility of developing new elements producing solutions with convergence patterns that cannot be stated *a priori*. Moreover, it is known that under certain circumstances the hybrid and mixed formulations can lead to the same solutions generated by a corresponding traditional conforming formulation (de Veubeke 1965, Stolarski 1987).

The recent developments in computer hardware, in particular in what concerns parallel processing, are forcing the finite element developers to reassess the competitiveness of the conventional formulation and to accept that the hybrid and mixed formulations, because of their higher flexibility, offer particular advantages within this new framework. Thus the renewed research interest on these non-conventional formulations, attested by the recent increase in the number of papers

† Professor
‡ Associate Professor

published in the specialised literature.

If this revival in the interest on the hybrid and mixed formulations is to succeed, it is essential to accept them as alternative concepts that should be developed *per se*, instead of insisting in establishing the bases for their development by mimicking the conforming approach. This is the philosophy adopted in the development of the hybrid finite element formulations reported here (Freitas 1989).

Four ingredients may be considered as the key aspects of this attempt to overcome the major drawbacks of the non-conventional formulations and thus provide the user with a much wider set of available finite element models:

- To depart from first principles of mechanics, namely equilibrium, compatibility and constitutive relations;
- To use nodeless, hierarchical approximation functions, thus removing the restrictions imposed by the use of nodal interpolations, extending the choice of available function bases and enhancing the implementation of adaptive procedures;
- To enforce energetically consistent definitions for the discrete generalised variables;
- To use mathematical programming concepts to recover the corresponding variational theorems and to establish the conditions for existence and uniqueness of solutions, from which the convergence characteristics of the models can be stated.

Two complementary sets of finite element models have been established from a Navier-type description of boundary value problems. They are termed *stress* and *displacement* models and are so designed as to generate, under certain conditions, statically and kinematically admissible solutions, respectively. For the sake of brevity, the displacement model is not covered in this paper.

Three alternative formulations can be stated for each finite element model, depending on the constraints enforced on the intervening approximation functions. The three alternative formulations for the *stress* model are the following:

- The *hybrid-mixed* formulation, for which the displacements (both in the domain and on the boundary of the finite elements) and the stresses are approximated independently but the corresponding functions are not required to satisfy locally the relevant field equations;
- The *hybrid* formulation, where the boundary displacements and the stresses are approximated independently and the latter are required to satisfy locally the differential equilibrium equations;
- The *hybrid-Trefftz* formulation, where now the stress approximation functions are constrained to satisfy locally the governing Beltrami-Michell equation, meaning they are associated with displacement fields that solve the governing Navier equation.

In every case the approximation criteria are so defined as to ensure consistency.

As the approach adopted here is not problem dependent, it is easily adaptable to distinct structural forms and alternative constitutive relations and is open to the incorporation of a wide variety of approximation functions.

In the latter part of the paper, different problems consisting in the analysis of plates and solids are used to illustrate the use of *digital functions, wavelets, standard, Legendre and Chebyshev polynomials,* as well as *trigonometric, hyperbolic and rational functions* as finite element approximation functions. Linear problems are used to support this illustration, as they combine formal simplicity with the ability to enhance the most relevant aspects of the alternative formulations.

2. Fundamental relations

The formulations are derived from *first principles*, that is the fundamental relations governing the boundary value problem under consideration, and not from equivalent variational statements.

The system of equations governing the linear response of an elastic body with domain V and boundary Γ, assigned to a Cartesian system of reference, can be stated as follows:

$$\boldsymbol{D}\boldsymbol{\sigma}+\boldsymbol{b}=\boldsymbol{0} \text{ in } V \tag{1}$$

$$\boldsymbol{\varepsilon}=\boldsymbol{D}^{*}\boldsymbol{u} \text{ in } V \tag{2}$$

$$\boldsymbol{\varepsilon}=\boldsymbol{f}(\boldsymbol{\sigma}-\boldsymbol{\sigma}_r)+\boldsymbol{\varepsilon}_r \text{ in } V \tag{3}$$

$$\boldsymbol{N}\boldsymbol{\sigma}=\boldsymbol{t}_\Gamma \text{ on } \Gamma_\sigma \tag{4}$$

$$\boldsymbol{u}=\boldsymbol{u}_\Gamma \text{ on } \Gamma_u \tag{5}$$

In the equilibrium condition Eq. (1), $\boldsymbol{\sigma}$ is the array where the independent components of the stress tensor are listed and vector $\boldsymbol{b}$ collects the components of the body forces. In the compatibility condition Eq. (2), vectors $\boldsymbol{\varepsilon}$ and $\boldsymbol{u}$ collect the independent components of the strain tensor and of the displacement vector.

In description Eq. (3) of the constitutive relations, the flexibility matrix $\boldsymbol{f}$ collects the relevant elastic constants, and vectors $\boldsymbol{\varepsilon}_r$ and $\boldsymbol{\sigma}_r$ are used to define residual strains and stresses.

The boundary conditions Eq. (4) and Eq. (5) apply to the entire limiting surface of the domain V under analysis: $\Gamma=\Gamma_\sigma\cup\Gamma_u$ and $\phi=\Gamma_\sigma\cap\Gamma_u$. In the static boundary condition Eq. (4), matrix $\boldsymbol{N}$ collects the components of the unit outward normal vector associated with the entries of the differential equilibrium matrix $\boldsymbol{D}$ and $\boldsymbol{t}_\Gamma$ is the vector that collects the tractions prescribed on portion Γ_σ of the enveloping surface. The kinematic boundary condition Eq. (5) states that displacements $\boldsymbol{u}_\Gamma$ are prescribed on the complementary portion Γ_u. The notation used above can accommodate mixed boundary conditions.

Appropriate combinations of the field Eqs. (1) to (3) yield the governing Navier equation,

$$\boldsymbol{D}\,\boldsymbol{k}\,\boldsymbol{D}^{*}\boldsymbol{u}+\boldsymbol{D}(\boldsymbol{\sigma}_r-\boldsymbol{k}\boldsymbol{\varepsilon}_r)+\boldsymbol{b}=\boldsymbol{0} \text{ in } V \tag{6}$$

where $\boldsymbol{k}$ is the elastic stiffness matrix:

$$\boldsymbol{k}=\boldsymbol{f}^{-1} \tag{7}$$

The basic properties of system Eqs. (1)-(5) are the following: the differential equilibrium and compatibility operators $\boldsymbol{D}$ and $\boldsymbol{D}^{*}$ are *linear* and *adjoint* in the context of geometrically linear models: the flexibility matrix $\boldsymbol{f}$ is *symmetric* and has *constant entries* when a linear, reciprocal elastic law is assumed. To ensure consistency, the equivalent properties must be preserved in the finite element model.

3. Basic finite element approximations

In the *hybrid-mixed formulation* the displacements and the stresses in the domain V of the element are independently approximated in each finite element, as stated by Eqs. (8) and (9) in Table 1, where matrices $\boldsymbol{S}_V$ and $\boldsymbol{U}_V$ collect appropriate approximation functions, vectors $\boldsymbol{X}$ and $\boldsymbol{q}_V$ list the associated weights and vectors $\boldsymbol{\sigma}_p$ and $\boldsymbol{u}_p$ are used to model particular solutions,

Table 1 Finite element approximations and associated dual variables for the hybrid-mixed stress model

$\sigma = \boldsymbol{S}_V \boldsymbol{X} + \sigma_p$ in V	(8)	$\boldsymbol{u} = \boldsymbol{U}_V \boldsymbol{q}_V + \boldsymbol{u}_p$ in V	(9)	$\boldsymbol{u} = \boldsymbol{U}_\Gamma \boldsymbol{q}_\Gamma$ on Γ_σ	(10)
$\boldsymbol{e} = \int \boldsymbol{S}_V^t \varepsilon \, dV$	(11)	$\boldsymbol{Q}_V = \int \boldsymbol{U}_V^t \boldsymbol{b} \, dV$	(12)	$\boldsymbol{Q}_\Gamma = \int \boldsymbol{U}_\Gamma^t \boldsymbol{t}_\Gamma \, d\Gamma_\sigma$	(13)
$\boldsymbol{X}^t \boldsymbol{e} = \int (\sigma - \sigma_p)^t \varepsilon \, dV$	(14)	$\boldsymbol{q}_V^t \boldsymbol{Q}_V = \int (\boldsymbol{u} - \boldsymbol{u}_p)^t \boldsymbol{b} \, dV$	(15)	$\boldsymbol{q}_\Gamma^t \boldsymbol{Q}_\Gamma = \int \boldsymbol{u}^t \boldsymbol{t}_\Gamma \, d\Gamma_\sigma$	(16)

for instance those associated with body forces, specific boundary conditions or residual stresses and strains. In general, it is convenient to construct the approximation basis from a complete set of functions.

In the stress model, the displacements are also approximated on the static boundary of the element in form Eq. (10), where matrix $\boldsymbol{U}_\Gamma$ collects the boundary approximation functions and vector $\boldsymbol{q}_\Gamma$ the corresponding weights. It should be noted that, for a free element, the definition of the static boundary Γ_σ is relaxed to include all the boundaries where on the displacements are not prescribed.

Also given in Table 1 are the definitions for the *generalised strains*, $\boldsymbol{e}$, the *generalised body forces*, $\boldsymbol{Q}_V$, and the *generalised tractions*, $\boldsymbol{Q}_\Gamma$, respectively associated with the generalised stresses, $\boldsymbol{X}$, and the generalised domain and boundary displacements, $\boldsymbol{q}_V$ and $\boldsymbol{q}_\Gamma$. They represent the dual transformations of the stress and displacement approximations Eq. (8) to Eq. (10), thus ensuring that the finite element discrete fields dissipate the same energy as the continuum fields they are associated with, as stated by Eqs. (14) to (16).

As it is shown below, this is a sufficient condition to ensure that the finite element models display the properties that typify the problem under analysis, namely:

- *Linearity*, that is finite element arrays with constant entries;
- *Static-kinematic duality*, meaning that the finite element equilibrium and compatibility matrices are the transpose of each other;
- *Constitutive reciprocity*, encoded by symmetric finite element elasticity matrices.

4. The hybrid-mixed stress model

The *generalised stresses*, $\boldsymbol{X}$, and the *generalised domain and boundary displacements*, $\boldsymbol{q}_V$ and $\boldsymbol{q}_\Gamma$, collect approximation weights that need not - and in general will not - correspond to nodal or modal values: the physical concepts of node and mode are herein avoided to release unnecessary constraints in the selection of approximation functions collected in matrices $\boldsymbol{S}_V$, $\boldsymbol{U}_V$ and $\boldsymbol{U}_\Gamma$. In general, it will be convenient to construct the approximation bases from complete sets of functions.

Moreover, besides linear independency, in the hybrid-mixed stress model the functions present in the finite element approximations Eq. (8) to Eq. (10) are not required to satisfy any of the relevant fundamental relations Eq. (1) to Eq. (5):

- The stress fields collected in matrix $\boldsymbol{S}_V$ need not satisfy either the equilibrium condition Eq. (1) or the static boundary condition Eq. (4);

Table 2 Finite element equations for the hybrid-mixed stress model

Statics (17)	Kinematics (18)	Elasticity (19)
$\begin{bmatrix} -A_V^t \\ A_\Gamma^t \end{bmatrix} X = \begin{Bmatrix} Q_V + Q_{Vp} \\ Q_\Gamma - Q_{\Gamma p} \end{Bmatrix}$	$e = [-A_V \ A_\Gamma] \begin{Bmatrix} q_V \\ q_\Gamma \end{Bmatrix} + e_\Gamma - e_{Vp}$	$e = F_V X + e_{Vr}$

- Also, neither the strains compatible with the displacements U_V nor the elastic strains associated with the stresses S_V are explicitly used, meaning that neither the compatibility condition (2) nor the elastic constitutive relations Eq. (3) are locally satisfied;
- Lastly, the boundary displacement approximation functions listed in matrix U_Γ are not required to satisfy continuity conditions.

The finite element basic relations for the hybrid-mixed stress model are summarised in Table 2.

Definition Eq. (11) for the generalised strains is used to enforce the local compatibility condition (2) on a Galerkin-weighed residual form, using the stress approximation functions as weighing functions,

$$\int S_V^t (\varepsilon - D^* u)\, dV = 0 \tag{20}$$

or:

$$e = \int S_V^t (D^* u)\, dV \tag{21}$$

To derive the finite element description (18) for Kinematics, Eq. (21) is first integrated by parts to mobilise the boundary terms and thus enable the combination of the kinematic admissibility conditions (2) and (5) in a single statement:

$$e = -\int (DS_V)^t u \, dV + \int (NS_V)^t u \, d\Gamma_\sigma + \int (NS_V)^t u_\Gamma d\Gamma_u \tag{22}$$

Inserting above the displacement approximations (9) and (10), the following expressions are found for the finite element compatibility matrix and for the terms associated with prescribed displacements:

$$A_V = \int (D\,S_V)^t U_V dV \tag{23}$$

$$A_\Gamma = \int (N\,S_V)^t U_V d\Gamma_\sigma \tag{24}$$

$$e_{Vp} = \int (D\,S_V)^t u_p dV \tag{25}$$

$$e_\Gamma = \int (N\,S_V)^t u_\Gamma d\Gamma_u \tag{26}$$

Similarly, definitions (12) and (13) for the generalised body forces and boundary tractions are used to enforce the local equilibrium condition (1) and the static boundary condition (4), respectively, on a Galerkin-weighed residual form, using now as weighing functions the displacement approximation functions in the domain and on the boundary of the element:

$$\int \boldsymbol{U}_V^t(\boldsymbol{D}\,\sigma+\boldsymbol{b})\,dV=\boldsymbol{0} \tag{27}$$

$$\int \boldsymbol{U}_\Gamma^t(\boldsymbol{N}\,\sigma-\boldsymbol{t}_\Gamma)\,d\boldsymbol{\Gamma}_\sigma=\boldsymbol{0} \tag{28}$$

or

$$-\int \boldsymbol{U}_V^t(\boldsymbol{D}\,\sigma)\,dV=\boldsymbol{Q}_V \tag{29}$$

$$\int \boldsymbol{U}_\Gamma^t(\boldsymbol{N}\,\sigma)\,d\boldsymbol{\Gamma}_\sigma=\boldsymbol{Q}_\Gamma \tag{30}$$

The discrete description of Statics, given by Eq. (17) in Table 2, is obtained inserting in Eqs. (29) and (30) the stress approximation (8). Static-kinematic duality is preserved, as the finite element equilibrium matrices are the transpose of the domain and boundary compatibility matrices (23) and (24), respectively, and the following expressions are found for the terms associated with the prescribed stress field:

$$\boldsymbol{Q}_{Vp}=\int \boldsymbol{U}_V^t(\boldsymbol{D}\,\sigma_p)\,dV \tag{31}$$

$$\boldsymbol{Q}_{\Gamma p}=\int \boldsymbol{U}_\Gamma^t(\boldsymbol{N}\,\sigma_p)\,d\boldsymbol{\Gamma}_\sigma \tag{32}$$

Definition (11) for the generalised strains is also used to enforce the local elasticity condition (3) on a Galerkin-weighed residual form, using again the stress approximation functions as weighing functions,

$$\int \boldsymbol{S}_V^t[\varepsilon-\boldsymbol{f}(\sigma-\sigma_r)-\varepsilon_r]\,dV=0 \tag{33}$$

$$\boldsymbol{e}=\int \boldsymbol{S}_V^t[\boldsymbol{f}(\sigma-\sigma_r)+\varepsilon_r]\,dV \tag{34}$$

The discrete representation of Elasticity, given by Eq. (19) in Table 2, is obtained substituting the stress approximation (8) in Eq. (34), yielding definition Eq. (35) for the symmetric finite element flexibility matrix and definition (36) for the term associated with prescribed stresses and strains:

$$\boldsymbol{F}_V=\int \boldsymbol{S}_V^t\boldsymbol{f}\boldsymbol{S}_V\,dV \tag{35}$$

$$\boldsymbol{e}_{Vr}=\int \boldsymbol{S}_V^t[\boldsymbol{f}(\sigma_p-\sigma_r)+\varepsilon_r]\,dV \tag{36}$$

The results above show that the finite element Eqs. (17) to (19) can be interpreted as the Galerkin-weighed enforcement of the fundamental relations (1) to (5) consistent with the finite element approximations (8) to (10):

- The finite element description of Statics, Eq. (17), represents the $\boldsymbol{U}_V$- and the $\boldsymbol{U}_\Gamma$- weighed residual enforcement of the equilibrium condition (1) and of the static boundary condition (4), respectively;

- The finite element description of Kinematics, Eq. (18), represents the $\boldsymbol{S}_V$-weighed residual enforcement of the compatibility condition (2) wherein the kinematic boundary condition (5) is locally enforced;
- The finite element description of Elasticity, Eq. (19), represents the $\boldsymbol{S}_V$-weighed residual enforcement of the elasticity relations (3).

5. The hybrid stress model

The *hybrid stress* model is a direct specialisation of the hybrid-mixed model described above and is obtained by constraining the stress approximation (8) to satisfy locally the equilibrium condition (1):

$$\boldsymbol{D}\boldsymbol{S}_V=\boldsymbol{0} \text{ in } V \tag{37}$$

$$\boldsymbol{D}\sigma_p+\boldsymbol{b}=\boldsymbol{0} \text{ in } V \tag{38}$$

The constraints above restrict only marginally the bases from which the finite element approximations can be built up. The generation of self-equilibrated stress fields is implemented easily using appropriate stress potentials.

These constraints on the approximation bases are compensated by important practical gains:

- The stress approximation (8) satisfies locally the equilibrium condition, thus meeting *a priori* a necessary condition to obtain statically admissible finite element solutions;
- The displacements need no longer to be approximated in the domain of the element, which reduces the chances of generating approximation bases that induce spurious modes;
- All arrays present in the hybrid stress finite element description of Statics and Kinematics have boundary integral expressions;
- The number of degrees of freedom required to achieve an equivalent level of accuracy in the stress estimate is substantially lower than that required by the hybrid-mixed stress model.

Consequent upon constraint (37), the S_V-weighed residual enforcement (22) of the kinematic admissibility conditions (2) and (5) reduces to form,

$$\boldsymbol{e}=-\int(\boldsymbol{O})^t\boldsymbol{u}\,dV+\int(\boldsymbol{N}\boldsymbol{S}_V)^t\boldsymbol{u}\,d\Gamma_\sigma+\int(\boldsymbol{N}\boldsymbol{S}_V)^t\boldsymbol{u}_\Gamma d\Gamma_u \tag{39}$$

which shows that approximation (9) for the displacements in the domain of the element becomes irrelevant. The resulting finite element description for Kinematics simplifies to form (41), given in table 3. Definitions (24) and (26) still hold for the intervening finite element arrays.

Also consequent upon constraints (37) and (38), Eq. (27) is made redundant and the finite element description for Statics reduces to the $\boldsymbol{U}_\Gamma$-weighed enforcement (28) of the static boundary condition (4), as stated by Eq. (40) in Table 3.

The finite element description (42) for Elasticity is the same as that derived for the hybrid mixed stress model.

Table 3 Finite element equations for the hybrid stress model

Statics (40)	Kinematics (41)	Elasticity (42)
$A_\Gamma^t X = Q_\Gamma - Q_{\Gamma p}$	$e = A_\Gamma q_\Gamma + e_\Gamma$	$e = F_V X + e_{Vr}$

6. The hybrid-Trefftz stress model

The *hybrid-Trefftz* stress model is obtained by further constraining the stress approximation (8) to be associated with strain and displacement distributions that satisfy locally the compatibility and elasticity conditions (2) and (3), besides solving the equilibrium condition (1) through constraints (37) and (38).

This is equivalent to assume that the stress fields S_V and σ_p in approximation (8) derive from displacement functions, U_V and u_p,

$$S_V = k\, D^*\, U_V \text{ in } V \tag{43}$$

$$\sigma_p = k(D^*\, u_p - \varepsilon_r) + \sigma_r \text{ in } V \tag{44}$$

that represent, respectively, homogeneous and particular solutions of the Navier Eq. (6):

$$D\, k\, D^*\, U_V = O \text{ in } V \tag{45}$$

$$D k\, D^* u_p + D(\sigma_r - k\varepsilon_r) + b = 0 \text{ in } V \tag{46}$$

The constraints above have no direct consequence on the finite element description for Statics and Kinematics, which preserve expressions (40) and (41), as stated in Table 4. However, they are necessary to obtain the alternative description (49) for Elasticity, where now all the finite element arrays present boundary integral expressions, as it was already the case for the equilibrium and compatibility arrays.

Table 4 Finite element equations for the hybrid-Trefftz stress model

Statics (47)	Kinematics (48)	Elasticity (49)
$A_\Gamma^t X = Q_\Gamma - Q_{\Gamma p}$	$e = A_\Gamma q_\Gamma + e_\Gamma$	$e = F_\Gamma X + e_{\Gamma r}$

To obtain the new description for the finite element flexibility matrix, Eq. (43) is first inserted in definition (35),

$$F_V = \int S_V^t\, D^*\, U_V\, dV \tag{50}$$

and integration by parts is implemented next to enforce constraint Eq. (45), yielding the following alternative boundary integral expression:

$$F_\Gamma = \int (N S_V)^t\, U_V\, d\Gamma \tag{51}$$

Applying a similar procedure to definition (36) for the generalised residual strains, using now result (46), the alternative boundary expression thus found is the following:

$$e_{\Gamma r} = \int (N S_V)^t u_p d\Gamma \tag{52}$$

Constraints (43) to (46) restrict further the bases from which the hybrid-Trefftz stress elements can be derived. It should be noted, however, that the necessary function bases are available and well defined in the specialised literature for a wide range of structural forms and different constitutive relations. They are generally derived from displacement potentials constrained to satisfy the Navier equation or from stress potentials governed by the corresponding Beltrami equation.

The main features of the hybrid-Trefftz stress model can be summarised as follows.

• The stress approximation (8), besides satisfying locally the equilibrium condition, is now associated with elastic strain distributions and unique, compatible displacement fields:

$$\varepsilon = E_V X + \varepsilon_p \text{ in } V \tag{53}$$

$$u = U_V X + u_p \text{ in } V \tag{54}$$

- As in the hybrid stress model, the displacements are only approximated on the boundary of the element;
- All arrays present in the hybrid-Trefftz stress finite element model have boundary integral expressions;
- The number of degrees of freedom needed to achieve a level of accuracy equivalent to that produced by the hybrid stress model is substantially lower, as the hybrid-Trefftz estimates generate from local solutions of the governing equations;
- The finite element model is free of spurious modes.

7. Finite element solving systems

The elementary solving systems for the alternative stress models described above are summarised in Table 5. They are obtained combining the associated finite element descriptions of Statics, Kinematics and Elasticity given in Tables 2 to 4 to eliminate the generalised strains, e, as explicit

Table 5 Finite element solving systems

Hybrid-mixed stress model (55)
$\begin{bmatrix} F_V & A_V & -A_\Gamma \\ A_V^t & O & O \\ -A_\Gamma^t & O & O \end{bmatrix} \begin{Bmatrix} X \\ q_V \\ q_\Gamma \end{Bmatrix} = \begin{Bmatrix} e_\Gamma - e_{Vp} - e_{Vr} \\ -Q_V - Q_{Vp} \\ -Q_\Gamma + Q_{\Gamma p} \end{Bmatrix}$
Hybrid stress model (56)
$\begin{bmatrix} F_V & -A_\Gamma \\ -A_\Gamma^t & O \end{bmatrix} \begin{Bmatrix} X \\ q_\Gamma \end{Bmatrix} = \begin{Bmatrix} e_\Gamma - e_{Vr} \\ Q_{\Gamma p} - Q_\Gamma \end{Bmatrix}$
Hybrid-Trefftz stress model (57)
$\begin{bmatrix} F_\Gamma & -A_\Gamma \\ -A_\Gamma^t & O \end{bmatrix} \begin{Bmatrix} X \\ q_\Gamma \end{Bmatrix} = \begin{Bmatrix} e_\Gamma - e_{\Gamma r} \\ Q_{\Gamma p} - Q_\Gamma \end{Bmatrix}$

variables.

As the flexibility matrix (35) is positive-definite, system (55) can be condensed on the generalised displacements,

$$\begin{bmatrix} K_{VV} & -K_{VT} \\ -K_{VT}^t & K_{TT} \end{bmatrix} \begin{Bmatrix} q_V \\ q_\Gamma \end{Bmatrix} = \begin{Bmatrix} Q_V{}^* \\ Q_\Gamma{}^* \end{Bmatrix} \tag{58}$$

or further on the generalised boundary displacements, into the form typical of the displacement formulation:

$$K_V{}^* q_\Gamma = Q^* \tag{59}$$

The hybrid and hybrid-Trefftz systems (56) and (57) can be condensed into a similar form. Format (59) for the finite element solving system is often used to extend to hybrid elements the libraries of the commercial finite element codes based on conforming, displacement elements, simply by implementing the boundary displacement approximation (10) on a nodal frame basis.

The governing system of a structure discretised into elements is obtained by assembling one of the alternative elementary systems defined above by requiring adjacent elements to share the same boundary displacement approximation law (10). The assembled finite element governing systems present a structure that is similar to that of the elementary systems they generate from, as given in Table 5 or, alternatively, by Eqs. (58) and (59).

The assemblage procedure of the finite element solving systems given in table V consists, therefore, in the implementation of simple, direct allocation operations, that do not involve the superposition of the contributions of connecting elements typical of the conventional displacement formulation. The entries of vector Q_Γ associated with the inter-element boundary tractions are set to zero to model traction continuity. These entries are computed from definition (13) for the actual, prescribed tractions on the assembled finite element mesh.

The assemblage procedure described above can be generalised to allow for independent boundary displacement approximation laws along adjacent elements (Almeida 1991). A basically similar technique is used to combine stress and displacement elements in the same finite element mesh (Rebelo, 1993).

8. Numerical Implementation

The governing systems summarised in Table 5 display a special structure that must be conveniently exploited in the phase of numerical implementation. The following aspects are particularly relevant:

- The solving systems are symmetric and sparse, as it is typical of all finite element solving systems;
- The dimension of the solving systems for hybrid-mixed elements is relatively high but this limitation is compensated by the high sparsity index of the system, consequent upon the block-diagonal structure of the flexibility matrix;
- The sparsity index of the solving systems for the hybrid-mixed stress model is further improved by the use of orthogonal approximation functions;
- A significant number of the finite element arrays, in fact all arrays in the hybrid-Trefftz model, present boundary integral expressions, a feature typical of the boundary element

method;

- The use of coarse finite element meshes based on few but very rich elements and the implementation of adaptive techniques is possible and simple to implement as hierarchical series are used to construct the finite element approximation bases;
- Numerical integration can be minimised or even fully avoided, in particular for the hybrid-mixed and hybrid models, as the simplicity of the approximation functions allow for the direct encodement of the analytical expressions of the finite element arrays;
- The generalised tractions, $\boldsymbol{q}_\Gamma$, are the only variables that can be shared, as all the remaining variables used to describe the approximations in the domain of the elements, the generalised displacements and stresses, $\boldsymbol{q}_V$ and $\boldsymbol{X}$, are strictly element dependent;
- The post-processing phase is substantially simplified as the stress and displacement fields can be directly computed from the finite element solution using definitions (8) and (9) for the hybrid-mixed model and definitions (8) and (54) for the hybrid-Trefftz elements, respectively;
- The independent displacement estimates obtained from the boundary approximation (10) can be used directly to assess the convergence of the solution;
- The graphic representation of the finite element solutions is also simplified because the field and boundary approximations are strictly element dependent and smoothing techniques need not to be applied as highly accurate solutions can be obtained using high degree, hierarchical approximation functions.

Highly efficient finite element codes can be implemented by exploiting conveniently the features above, in particular when parallel processing is used (Almeida 1996).

Different approximation functions have been tested, namely digital Walsh functions and wavelets (Freitas 1992 and Castro 1996), orthogonal and non-orthogonal polynomials (Almeida 1991 and Pereira 1996) and fundamental solutions for elastostatic problems, such as trigonometric (Freitas 1991), hyperbolic, exponential and logarithmic functions (Freitas 1996). Examples of one dimensional Walsh functions (Walsh 1923) and wavelets (Daubechies 1988) are given in Figs. 1 and 2.

Hybrid-mixed and hybrid-stress formulations have been developed for 2-D problems (Almeida 1991, Freitas 1996c), 3-D problems (Almeida 1996b) and for the analysis of Mindlin (and higher-

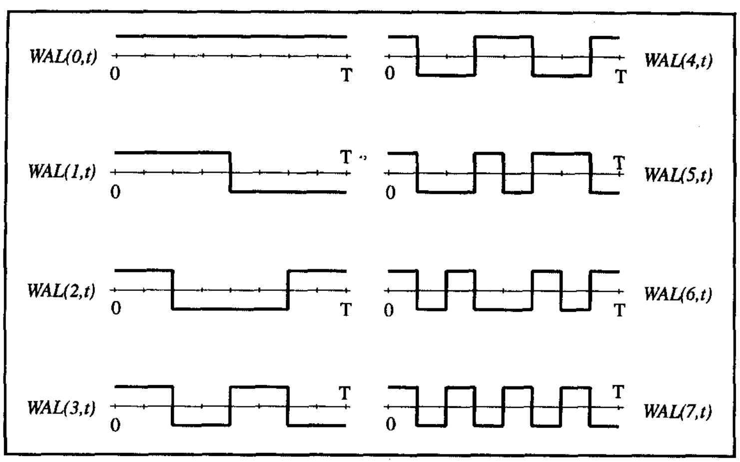

Fig. 1 One dimensional Walsh functions.

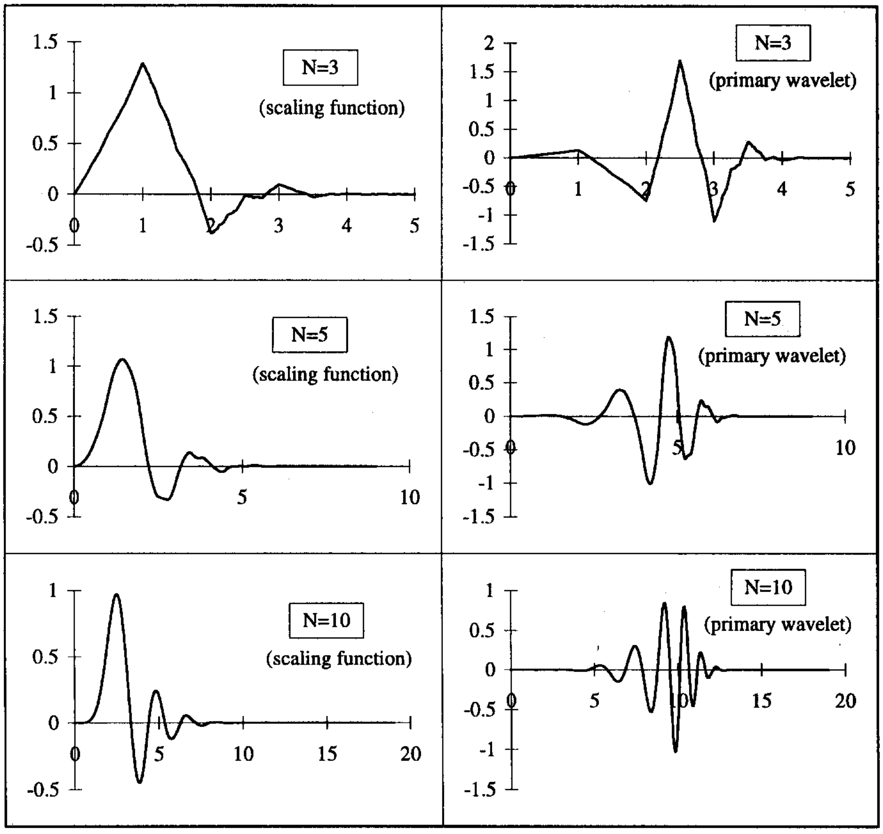

Fig. 2 One dimensional scaling functions and primary wavelets.

order) bending plates (Pereira 1996b) and used to model interlaminar stresses in composite laminates (Pereira 1993). Both hybrid-mixed (Almeida 1989, Castro 1996) and hybrid-stress (Almeida 1989, 1995) formulations have been applied to the elastoplastic analysis of 2-D problems. The experience with hybrid-Trefftz formulations is limited to quasi-static (Freitas 1996a, 1996b) and dynamic elastic problems (Freitas 1996d).

The governing systems associated with the hybrid-Trefftz formulations are small in dimension, positive semi-definite and well conditioned. The efficiency that can be attained in the storage and solution of such systems is countered by the implementation of the heavy procedures required to process the singular functions that may be present in the (boundary integral) definitions of the structural operators. Analytical and semi-analytical, special purpose procedures seem to be the natural way to overcome this difficulty, exploiting the currently available symbolic processing programs.

Large systems and the threat of spurious modes is the price paid to achieve the high malleability that typifies the hybrid-mixed and, to a lesser extent, the hybrid stress models. Static spurious modes are absent from these formulations as the stress approximation functions are linearly independent. The existence of kinematic spurious modes can be minimised by establishing appropriate relations on the degrees of the intervening approximation functions. The use of assemblies of elements for which the spurious kinematic modes are eliminated at macro-element level is another approach to handle this problem (Maunder 1996). Alternatively, dependent equations

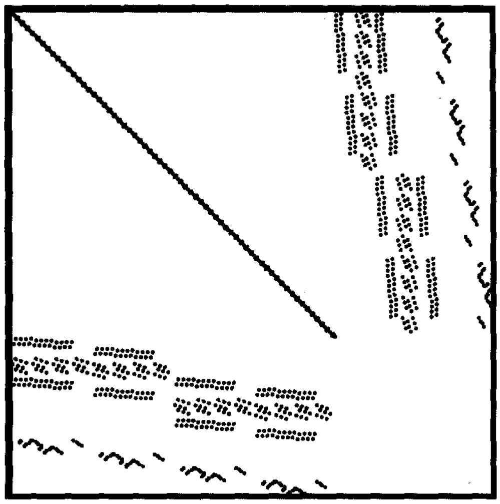

Fig. 3 Typical pattern of the governing system.

must be discarded during the solution of the governing system.

As closed form solutions for the structural operators can be obtained, setting up the governing system is, in general, a low cost operation. The use of orthogonal approximation functions allows for the generation of highly sparse systems, which can be stored and solved using appropriate algorithms (Harwell 1993 and Pissanetzky 1984). A typical pattern of the corresponding matrices is shown in Fig. 3.

9. Existence and uniqueness of solutions

It is important, from both theoretical and computational stand points, to establish clearly the sufficient conditions for the existence and uniqueness of the finite element solutions. This has been achieved in a consistent and formally elegant way for alternative structural analysis and optimisation problems using mathematical programming theory (Maier 1982 and Maier 1986).

The finite element systems given in Table 5 can be stated in the common form Eq. (60), using appropriate identifications for the system variables, x and y, as stated by Eq. (61) for the hybrid-mixed stress model and Eq. (62) for the hybrid and hybrid-Trefftz models, respectively:

$$\begin{bmatrix} -\boldsymbol{H} & \boldsymbol{M} \\ \boldsymbol{M}^t & \boldsymbol{G} \end{bmatrix} \begin{Bmatrix} \boldsymbol{x} \\ \boldsymbol{y} \end{Bmatrix} = \begin{Bmatrix} \boldsymbol{y}_0 \\ \boldsymbol{x}_0 \end{Bmatrix} \tag{60}$$

$$\boldsymbol{x} \equiv \boldsymbol{X} \text{ and } \boldsymbol{y} \equiv (\boldsymbol{q}_V, \boldsymbol{q}_\Gamma) \tag{61}$$

$$\boldsymbol{x} \equiv \boldsymbol{X} \text{ and } \boldsymbol{y} \equiv \boldsymbol{q}_\Gamma \tag{62}$$

Under certain sufficiency conditions (Karush 1939, Kuhn 1951), system (60) is equivalent to either of the following pair of dual quadratic programs:

$$\text{Min } z = \frac{1}{2}\boldsymbol{x}^t\boldsymbol{H}\boldsymbol{x} + \frac{1}{2}\boldsymbol{y}^t\boldsymbol{G}\boldsymbol{y} - \boldsymbol{y}^t\boldsymbol{x}_0 \tag{63a}$$

$$\text{subject to: } \boldsymbol{M}\boldsymbol{y} - \boldsymbol{H}\boldsymbol{x} = \boldsymbol{y}_0 \tag{63b}$$

$$\text{Min } w=\frac{1}{2}\boldsymbol{x}'\boldsymbol{H}\boldsymbol{x}+\frac{1}{2}\boldsymbol{y}'\boldsymbol{G}\boldsymbol{y}+\boldsymbol{x}'\boldsymbol{y}_0 \tag{64a}$$

$$\text{subject to: } \boldsymbol{M}'\boldsymbol{x}+\boldsymbol{G}\boldsymbol{y}-\boldsymbol{x}_0 \tag{64b}$$

Eq. (60) is thus uncoupled into sub-systems Eqs. (63b) and (64b), which define the primal and dual constraint sets, respectively. Solutions of these sub-systems are said to be feasible solutions of the corresponding programs. Among all the primal and dual feasible solutions (63b) and (64b), the optimal solution, or solutions of the corresponding program are those that simultaneously minimise the associated objective function, z and w, as defined in statements (63a) and (64a), respectively. Under the equivalence conditions referred above, these optimal solutions are also the solutions of system (60).

The sufficient conditions for the existence and uniqueness of the finite element solutions are directly obtained by applying the relevant mathematical programming theorems (Cottle 1963, Kunzi 1966) to programs (63) and (64). They can be used to establish under which situations the finite element models may produce either static or kinematic multiple solutions. Based on this information, it is possible to state the sufficient conditions that must be met to avoid the emergence of these spurious modes. They are particularly simple to implement in the development of hybrid-Trefftz elements.

10. Static and kinematic admissibility conditions

Let n_X, n_{qV} and $n_{q\Gamma}$ represent the number of degrees of freedom in the finite element stress and displacement approximations (8), (9) and (10), respectively. According to the equilibrium and compatibility conditions (17) and (18), given in Table 2, the static and the kinematic indeterminacy numbers of the hybrid-mixed stress element, α and β, are defined thus:

$$\alpha=n_X-n_{qV}-n_{q\Gamma}\geq 0 \tag{65}$$

$$\beta=n_{qV}+n_{q\Gamma} \tag{66}$$

The definitions above can be specialised for the hybrid and hybrid-Trefftz elements by letting $n_{qV}=0$.

The finite element solutions satisfy on average (weak enforcement) the static admissibility conditions (1) and (4) and the kinematic admissibility conditions (2) and (5); in general they do not satisfy locally these conditions (strong enforcement).

Definition (65) shows that the smaller is the static indeterminacy number of the stress element, the stronger is the enforcement of the static admissibility condition. As it is always possible to choose an approximation basis that implements this condition strongly, it may be stated that the finite element stress model may produce statically admissible solutions. However, and in consequence of the same definition, the enforcement of the kinematic admissibility conditions in formats (18), (41) or (48) is, in general, weak.

11. Energy statements and qualification of solutions

The finite element formulations are frequently derived from alternative energy statements, namely the virtual work Eq. (67) and stationary conditions on the potential energy (68), the complementary potential energy (69) and the Hellinger-Reissner (70) functionals:

$$\int \sigma^t \varepsilon dV = \int b^t u \, dV + \int t_\Gamma^t u \, d\Gamma_\sigma + \int u_\Gamma^t t \, d\Gamma_u \tag{67}$$

$$\Pi = \frac{1}{2}\int (\sigma + \sigma_r)^t (\varepsilon - \varepsilon_r) \, dV - \int b^t u \, dV - \int t_\Gamma^t u \, d\Gamma_\sigma \tag{68}$$

$$\Pi_* = \frac{1}{2}\int (\sigma + \sigma_r)^t (\varepsilon + \varepsilon_r) \, dV - \int u_\Gamma^t t \, d\Gamma_u \tag{69}$$

$$\Pi_{HR} = -\Pi_* - \int u^t (D\sigma + b) \, dV + \int u^t (t - t_\Gamma) \, d\Gamma_\sigma \tag{70}$$

Note that in definitions (68) and (69) the residual stress and strain fields satisfy, by definition, the following zero-dissipation condition:

$$\int \sigma_r^t \varepsilon_r dV = 0 \tag{71}$$

It can be shown that the inner product of equilibrium and compatibility conditions given in Tables 2, 3 and 4 for the alternative stress models recovers the virtual work Eq. (67). For instance, for the hybrid-mixed model this inner product yields the following result:

$$q_\Gamma^t (Q_\Gamma - Q_{\Gamma p}) + q_V^t (Q_V + Q_{Vp}) = X^t (e - e_\Gamma + e_{Vp}) \tag{72}$$

To recover the virtual work equation it suffices to substitute in the equation above the definitions summarised in Table 1.

Taking into account the identifications (61) and (62), and recalling the expressions found for the equilibrium and compatibility conditions given in Tables 2, 3 and 4 for the alternative stress models, it can be easily found that the primal and dual feasible solutions (63b) and (64b) represent (weak) kinematically and statically admissible finite element solutions, respectively.

Identifications (73) and (74) for the primal and dual objective functions z and w are obtained substituting in their expressions the definitions found for the relevant matrices and vectors intervening in the governing systems (55) to (57) of the hybrid-mixed, hybrid and hybrid-Trefftz stress models, for the identifications (61) and (62), respectively, and manipulating next the resulting equations using the expressions found for the finite element arrays:

$$z = \Pi + constant \tag{73}$$

$$w = \Pi_* + constant \tag{74}$$

It is thus found that the primal and dual programs (63) and (64) encode the theorems on the minimum potential energy (68) and co-energy (69), respectively.

Under the same sufficiency conditions (Karush 1939, Kuhn 1951), the alternative pair of quadratic programs (75) and (76) is also equivalent to system (60):

$$\text{Min } z_* = -\frac{1}{2} x^t H x + \frac{1}{2} y^t G y + x^t M y - x^t y_0 - y^t x_0 \tag{75}$$

$$\text{Min } w_{*} = -\frac{1}{2}x^t \boldsymbol{H} x + \frac{1}{2}y^t \boldsymbol{G} y + x^t \boldsymbol{M} y \text{ subject to system (60)} \tag{76}$$

Program (75) enjoys the feature of being unconstrained, meaning that a *stationary* value of functional z_{*} recovers the solution set of the governing system (60). The following identification,

$$z_{*} = -\Pi_{HR} + constant \tag{77}$$

is obtained using a process similar to the one described above for functionals z and w. Again, as the constant terms do not interfere in the optimal values of the objective function, it can be stated that program (75) encodes the stationary condition on the Hellinger-Reissner functional (70).

The results presented above show clearly that the finite element stress models derived here directly from the fundamental state conditions (1) to (5) are consistent with the relevant energy theorems of elastostatics. Therefore, these energy theorems could also be used to derive directly the finite element systems summarised in Table 5.

12. Numerical Illustrations

Typical applications in linear elastostatics are presented below for the hybrid-mixed, hybrid and hybrid-Trefftz finite element models. The graphic outputs shown for the distributions of stresses are directly obtained from computed values (Almeida 1992). No smoothing is applied.

The uniformly loaded triangular wedge, represented in Fig. 4, is studied using a Legendre polynomial approximation of degree 10. In table VI the values of the stresses at the points indicated are compared with those obtained by (Pian and Wu 1988) and (Dong and Freitas 1993). Fig. 5 shows the corresponding stress trajectories.

The same formulation is adopted in the implementation of the higher-order model used in the analysis of composite plates, where the 3D model is replaced by a sequence of 2D problems

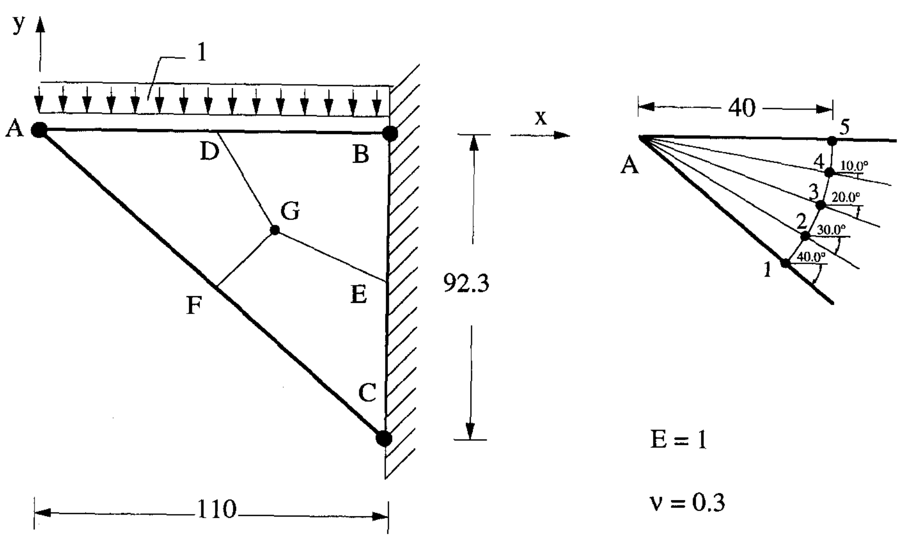

Fig. 4 Triangular wedge.

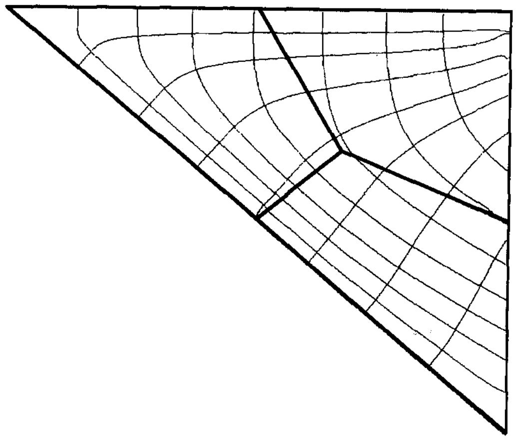

Fig. 5 Stress trajectories for the triangular wedge.

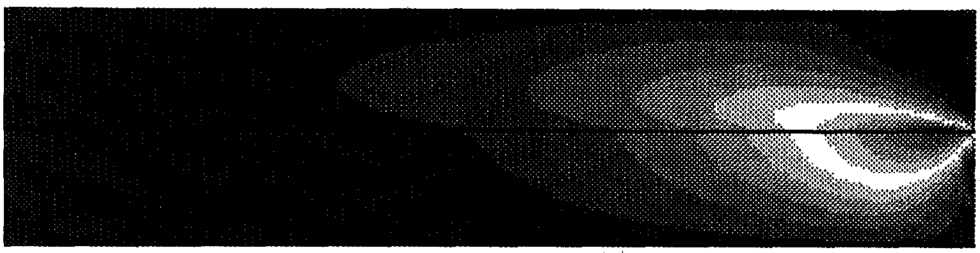

Fig. 6 Shear stress distribution in a cross-ply laminate (1/8 of specimen).

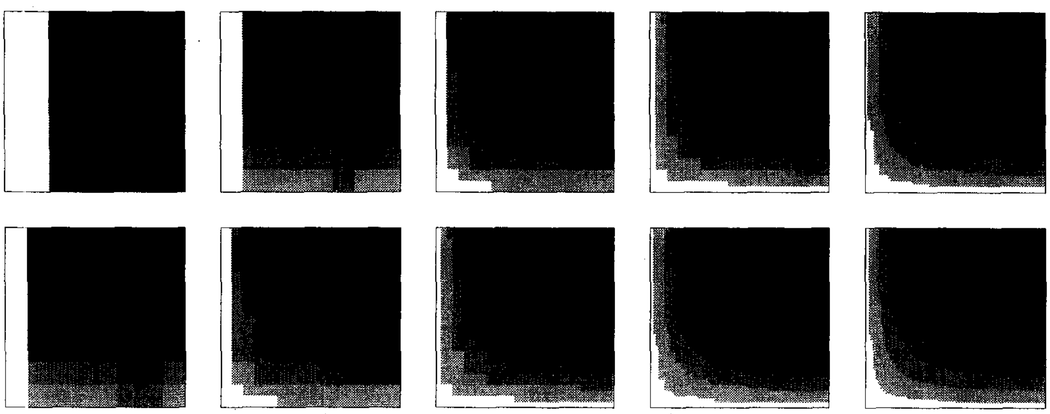

Fig. 7 Normal bending moments in a 1/4 of a thick plate subject to uniform load.

by expanding the displacement field on a power series on the thickness co-ordinate. Represented in Fig. 6 is the interlaminar shear stress concentration in a cross-ply laminate subject to uniform axial deformation.

Fig. 7 illustrates the convergence of the bending moment distributions in one quarter of a square, simply supported (hard) Mindlin plate, subject to uniform load. Two meshes are tested (A and B, with 1×1 and 2×2 square elements, respectively) with up to 2^p Walsh approximation functions, for each variable, in each direction.

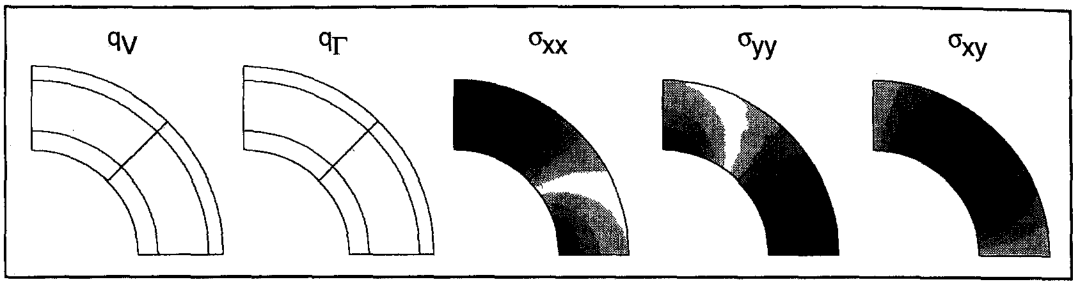

Fig. 8 Stresses and deformed shapes in a thick circular tube.

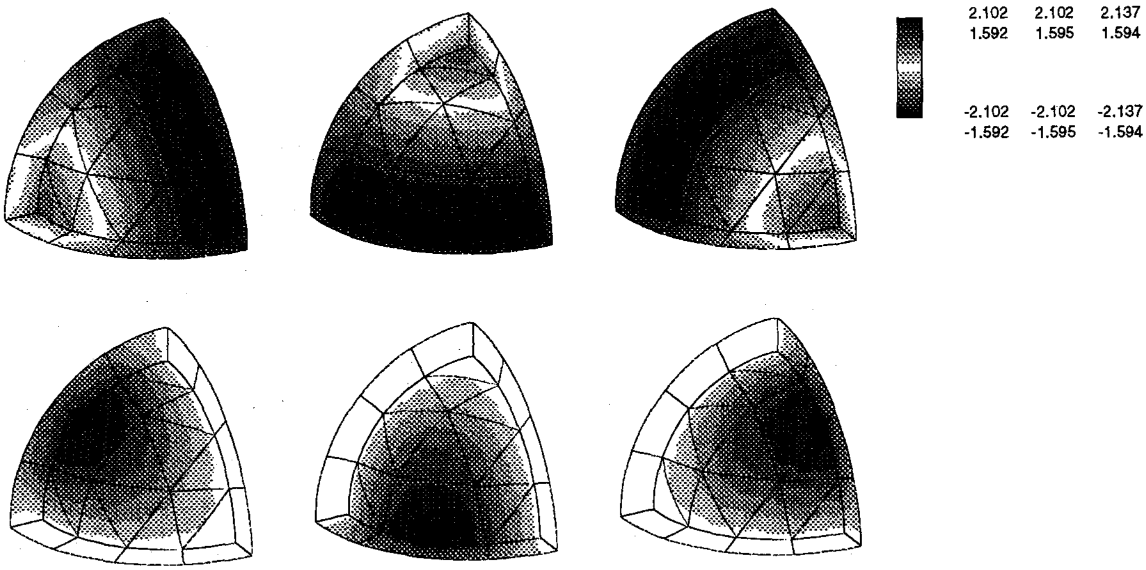

Fig. 9 Cartesian stresses in a thick shell under internal pressure (1/8 of the shell).

Wavelet approximation functions are used to obtain a solution for an infinite thick cylindrical tube subject to external pressure. The plane components of stress and the deformed shape of a cross section are represented in Fig. 8, when 8 translations of a wavelet with $N=10$ are used.

The results described above are solved using the hybrid-mixed stress model. The following two applications derive from the implementation of the hybrid stress model.

Solid elements, using polynomial approximation functions derived from the Morera stress potentials, are applied in the example of Fig. 9, where the Cartesian components of stress in this thick shell subject to internal pressure are represented.

An important characteristic of the hybrid stress model being described is the lack of compatibility in the resulting deformed shapes. The tapered plate under compression shown in Fig. 10 is used to illustrate this effect. The convergence of the non-conforming deformed shapes is presented in Fig. 11. Robust macro-elements free from spurious kinematic modes are used in the analysis (Ramsay 1995).

The illustration in Fig. 13 represents the stress patterns obtained with the hybrid-Trefftz stress model in the simulation of the elastic response of the stretched plate with a kinked crack shown in Fig. 12 ($\sigma=10$, $E=2$, 100, $\nu=0.3$, $L=w$, $a=w/4$, $l=w/100$, $w=4$). A relatively coarse finite

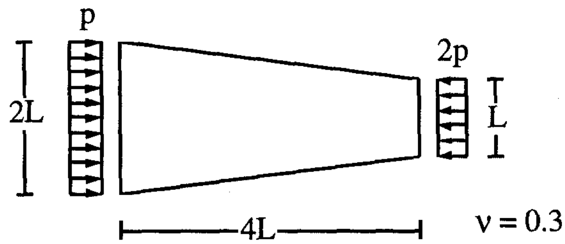

Fig. 10 Tapered plate subject to compression.

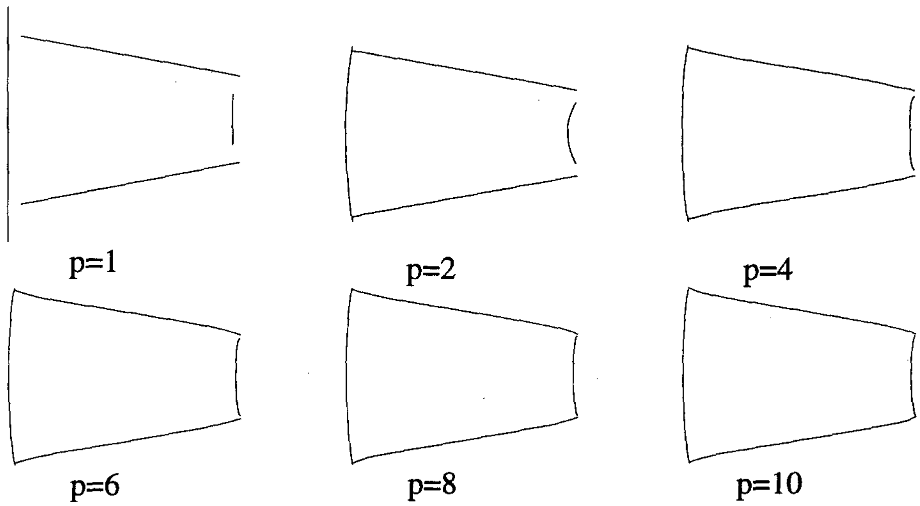

Fig. 11 Example of *p*-convergence for non-conforming deformed shapes.

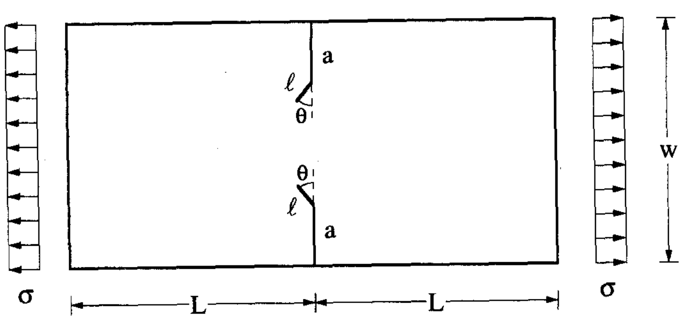

Fig. 12 Rectangular plate with kinked crack, subject to axial tension.

element mesh is adopted. Less than 200 degrees of freedom are sufficient to generate an accurate solution. In each element the stress field is approximated with Chebyshev polynomials satisfying the governing Navier equation. In the elements where cracks develop, the Chebyshev rational functions simulating exactly the local singular stress fields are directly injected in the crack kink and tip. The weight of these stress modes represent directly the crack stress intensity factors.

The last example is selected to illustrate the accuracy that can be achieved in the direct computation of stress intensity factors. The test shown in Fig. 14 has been devised to assess the effect of small cracks on the stress intensity factor of a major neighbouring crack ($L=3w$, $a=0.5w$,

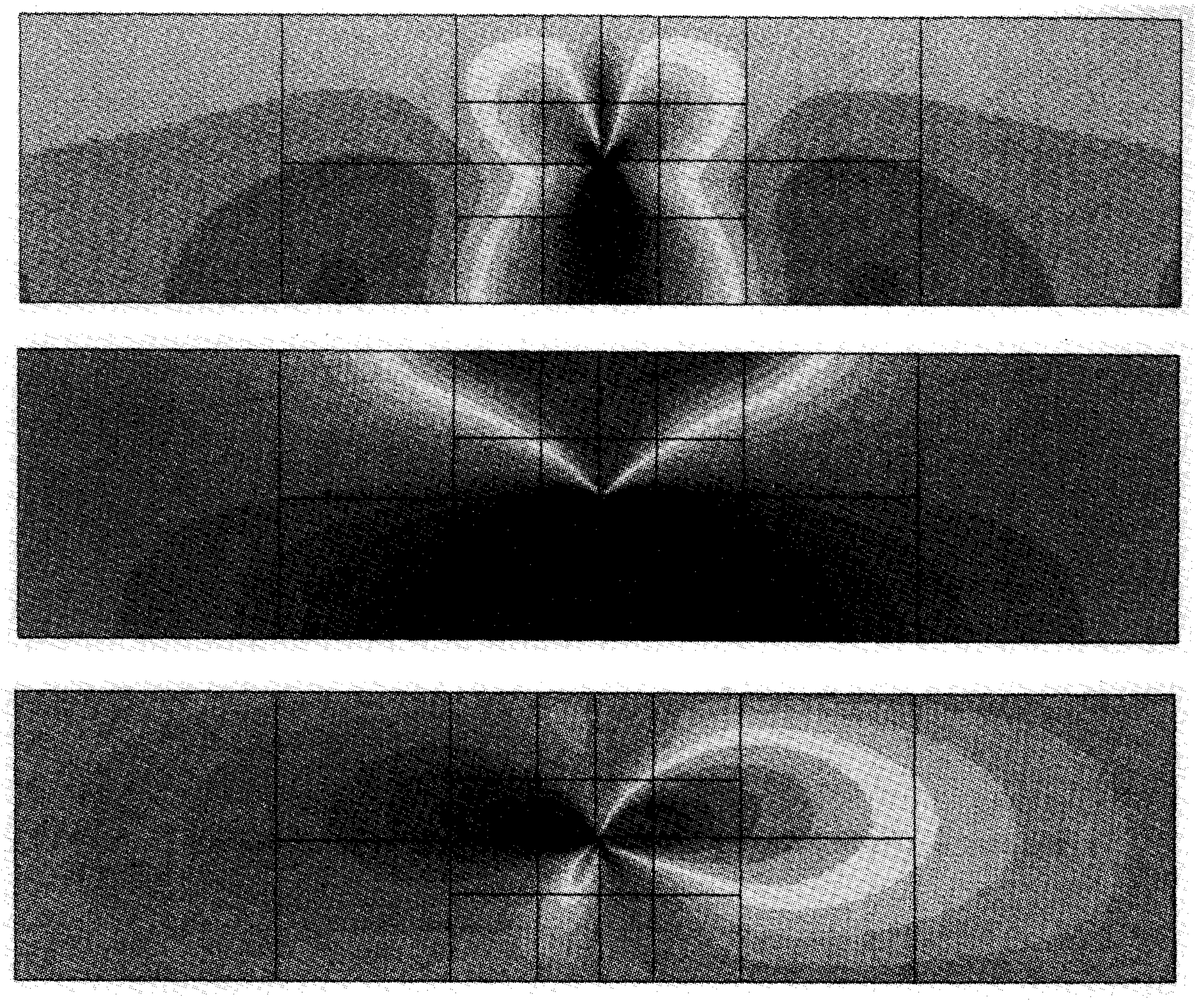

Fig. 13 Stress fields in the plate with the kinked crack.

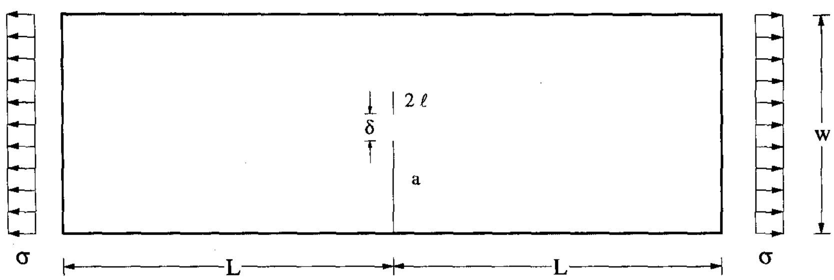

Fig. 14 Elastic plate with neighbouring cracks subject to axial tension.

$\delta = 0.025w$, $w = 10$). The results obtained on a 14 element mesh with the formulation described here (Freitas 1996) are given in Table 7 and shown in Fig. 15, where the stress intensity factors are normalised with respect to the mode I factor found for the plate in the absence of the microcrack, $K_{I0} = 158.6$.

Table 6 Stresses in the uniformly loaded plane wedge

		Pol	Pian-I	Pian-II	Dong
	σ_{xx}	−3.483	−2.220	−3.290	−3.499
1	σ_{yy}	−2.429	−1.850	−2.860	−2.463
	σ_{xy}	3.002	–	–	2.936
	σ_{xx}	−1.819	−1.590	−1.700	−1.830
2	σ_{yy}	−1.663	–	–	−1.652
	σ_{xy}	1.775	–	–	1.775
	σ_{xx}	0.303	1.010	0.500	0.201
3	σ_{yy}	−1.2045	–	–	−1.204
	σ_{xy}	0.826	–	–	0.825
	σ_{xx}	2.499	2.770	2.570	2.499
4	σ_{yy}	−1.027	–	–	1.028
	σ_{xy}	0.206	–	–	0.207
	σ_{xx}	4.924	2.95	4.270	4.943
5	σ_{yy}	−1.000	–	–	−1.000
	σ_{xy}	0.000	–	–	0.000

Table 7 Estimates for the stress intensity factor K_I

δ/l	0.250	0.400	0.666	1.000	2.000
Model 3	225.52	200.90	181.86	171.90	162.63
Model 4	236.74	210.04	188.45	176.83	165.10
Hybrid-Trefftz	228.00	204.58	185.18	174.08	163.62

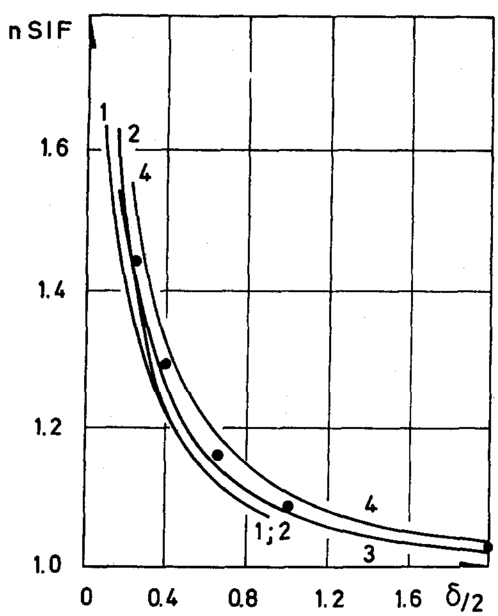

Fig. 15 Normalised stress intensity factor ($nSIF = K_I/K_{I0}$).

In Fig. 15, the results assigned to models 1 and 2 correspond to the solutions given in (Chudnovski 1983) and (Kachanov 1986), respectively. The results for models 3 and 4 are quoted from (Maiti 1992), respectively obtained with Maitis one point singularity element and the Dutta-Maiti-Kakodkar singularity element.

13. Closure

The solutions obtained with the hybrid/mixed finite element models described here are computationally competitive and can provide accurate and stable estimates for the response of structures.

The formulations suggested are particularly well suited for the development of adaptive methods as hierarchical approximation functions are easily incorporated. They are also appropriate to model stress concentration patterns developing in fracture mechanics problems, using suitable singular approximation functions. Their natural ability to implement higher-order plate and shell formulations can be exploited to establish efficient codes capable of simulating accurately interlaminar stresses developing in laminated structures.

These features follow from the open architecture that can be achieved by deriving the formulations from first principles, while being prepared to approximate a wide variety of fields (within a well defined set of consistency criteria) and to release conceptual constraints dictated by an overly rigid physical interpretation of the finite element method, of which the node and mode concepts are typical examples.

Another important characteristic is the possibility of obtaining direct bounds of the solution error and error estimators using pairs of statically and kinematically admissible solutions.

A common property of these formulations is the economy that they allow at both pre- and post-processing phases. They can operate accurately using coarse meshes of super finite elements, demanding the handling of small data structures, and are based on the direct approximation of different fields, allowing for efficient graphic representation of deformed shapes and strain and stress patterns.

Expert processing of (not necessarily definite) very large sparse systems becomes vital to achieve acceptable levels of numerical efficiency. The current developments in supercomputing, particularly in the area of parallel processing, open a wide and promising new field.

The conjugation of structural mechanics with mathematical programming yields immediate benefits from both theoretical and numerical standpoints. The energy theorems can be obtained a posteriori by identification of the mathematical programs associated with the structural governing system. Mathematical programming theory can also be used to establish sufficient conditions for the existence, uniqueness and stability of solutions. Lastly, efficient solution procedures can be developed by adapting mathematical programming algorithms to the physics specific to the structural problem under analysis.

Acknowledgements

Dr. A. Ramsay, Mr. L.M.S.S. Castro and Mr. O.J.B.A. Pereira participate in the supporting project. This work is part of the research activity of Instituto da Construção/IST and has been partially sponsored by program PRAXIS XXI research project PRAXIS/2/2.1/CEG/33/94 and by the European Commission through Human Capital and Mobility Network ERB4050PL1930382.

References

Almeida, J.P.M. (1991), "Modelos de elementos finitos para a anaise elastoplática", Ph.D. Thesis, Universidade Técnica de Lisboa.

Almeida, J.P.M. (1991), "Alternative approach to the formulation of hybrid equilibrium finite elements", *Comp. & Struct.*, **40**, 1043-1047.

Almeida, J.P.M. (1992), "Janela: uma interface gráfica destinada à aplicacão em problemas de Mecânica Computacional", *Internal Report, IST,* Lisbon.

Almeida, J.P.M. and Freitas, J.A.T. (1995), "Equilibrated or compatible finite element solutions in the elastoplastic analysis of stretching plates", *COMPLAS V,* 2071-2080, Barcelona.

Almeida, J.P.M., and Freitas, J.A.T. (1996), "On the parallel implementation of non-conventional finite element formulations", M. Papadrakakis, ed., *Advanced Finite Element Solution Techniques,* CIMNE, Barcelona, **39**, 3175-3194.

Almeida, J.P.M. and Pereira, O.J.B.A. (1996), "A set of hybrid equilibrium finite element models for the analysis of three-dimensional solids", *Int. J. Num. Meth. Engng.,* **39**, 2789-2802.

Castro, L.M.S.S. and Freitas, J.A.T. (1996), "Hybrid-mixed finite element elastoplastic analysis based on Walsh and wavelet interpolation", M. Papadrakakis, ed., *Advanced Finite Element Solution Techniques,* CIMNE, Barcelona, in press.

Chudnovsky, A. and Kachanov, M. (1983), "Interaction of a crack with a field of microcracks", *Int. J. Eng. Sci.,* **21**, 1009-1018.

Cottle, R.W. (1963), "Symmetric dual quadratic programs", *Q. Appl. Maths.,* **21**, 237-241.

Daubechies, I. (1988), "Orthonormal bases of compactly supported wavelets", *Comm. on Pure & Appl. Mathematics,* **41**, 906-996.

de Veubeke, B.F. (1965), "Displacement and equilibrium models in the finte element method", in *Stress Analysis,* ed. by O.C. Zienckiewicz and G.S. Holister, Wiley, London, 145-196.

Dong, Y.F. and Freitas, J.A.T. (1993), "Alternative approach for hybrid stress elements with incompatible displacements", CIVILCOMP93, Edinburgh, 99-105.

Freitas, J.A.T. (1989), "Duality and symmetry in mixed integral methods of elastostatics", *Int. J. Num. Meth. Engng.,* **28**, 1161-1179.

Freitas, J.A.T. and Pereira, E.M.B.R. (1991), "Application of the Mathieu series to the boundary integral method", *Comp. & Struct.,* **40**, 1307-1314.

Freitas, J.A.T. and Castro, L.M.S.S. (1992), "Digital interpolation in mixed finite element structural analysis", *Comp. & Struct.,* **44**, 743-751.

Freitas, J.A.T. and Ji, Z.-Y. (1996), "Hybrid-Trefftz boundary integral formulation for simulation of singular stress fields", *Int. J. Num. Meth. Engng.,* **39**, 281-308.

Freitas, J.A.T. and Ji, Z.-Y. (1996), "Hybrid-Trefftz equilibrium model for crack problems", *Int. J. Num. Meth. Engng.,* **39**, 569-584.

Freitas, J.A.T. and Castro, L.M.S.S. (1996), "Finite element solutions with Walsh series and wavelets", *CAMES,* in press.

Freitas, J.A.T. (1996), "Hybrid-Trefftz displacement and stress elements for elastodynamic analysis in the frequency domain", *CAMES,* in press.

Harwell Subroutine Library (1993), Release 11, Theoretical Studies Department, AEA Technology, Harwell.

Kachanov, M. (1986), "On crack-microcrack interactions", *Int. J. Fract.,* **30**, R65-R72.

Karush, W. (1939), "Minima of functions of several variables with inequalities as side conditions", M.S. Thesis, University of Chicago.

Kuhn, H.W. and Tucker, A.W. (1951), "Nonlinear Programming", *2nd Berkeley Symp. on Mathematical Statistics and Probability,* Berkeley.

Kunzi, H.P., Krelle, W. and Tucker, A.W. (1966), "Nonlinear Programming", Blaisdel.

Maier, G., and Munro, J. (1982), "Mathematical programming applications to engineering plastic analysis", *AM Update.*

Maier, G. and Smith, D.L. (1986), "Mathematical programming applications to engineering plastic analysis", *AM Update.*

Maiti, S.K. (1992), "A multicorner variable order singularity triangle to model neighbouring singularities", *Int. J. Numer. Meth. Engng.*, **35**, 391-408.

Maunder, E.A.W., Almeida, J.P.M. and Ramsay, A.C.A. (1996), "A general formulation of equilibrium macro-elements with control of spurious kinematic modes - The exorcism of an old curse", *Int. J. Num. Meth. Engng.*, **39**, 3175-3194.

Pereira, E.M.B.R. (1993), "Elementos finitos de tensão aplicados á análise elästica de estruturas, Ph.D. Thesis, Universidade Técnica de Lisboa.

Pereira, E.M.B.R. and Freitas, J.A.T. (1996), "A mixed-hybrid finite element model based on orthogonal functions", *Int. J. Num. Meth. Engng.*, **39**, 1295-1312.

Pereira, E.M.B.R. and Freitas, J.A.T. (1996), "Hybrid-mixed finite element model based on Legendre polynomials for Reissner-Mindlin plates", *Comp. Meth. Appl. Mech. Engng.*, in press.

Pian, T.H.H. and Tong, P. (1969), "Basis of finite element methods for solid continua", *Int. J. Num. Meth. Engng.*, **1**, 3-28.

Pian, T.H.H. and Wu, C.C. (1988), "A rational approach for choosing stress terms elements with incompatible displacements", *Int J Num Meth Engrng*, **26**, 2331-2343.

Pissanetzky, S. (1984), "Sparse matrix technology", Academic Press Inc.

Ramsay, A.C.A. (1995), "Robust variable degree equilibrium elements: their formulation and application", Report for Human Capital and Mobility Network, ERB4050PL1930382.

Rebelo, J.S. (1993), "Modelos de elementos finitos para a anáise elática de lajes, PhD Thesis, Universidade Técnica de Lisboa.

Stolarski, H. and Belytschko, T. (1987), "Limitation principles for mixed finite elements based on the Hu-Wahizu variational formulation", *Comp. Meth. Appl. Mech & Eng*, **60**, 195-216.

Walsh, J.L. (1923), "A closed set of orthogonal functions", *Ann. J. Math.*, **55**, 5-24.